

COMPARATIVE STUDY OF DFT AND DFT-D METHODS FOR ELECTRONIC AND OPTICAL PROPERTIES OF ZINC-BLENDE ZINC SULFIDE (zb-ZnS)

¹A. S. Olayinka and ²W.Nwankwo

¹Department of Physics, Edo University Iyamho, Edo State, Nigeria

²Department of Computer Science, Edo University Iyamho, Edo State, Nigeria

Abstract

Structural, electronic and optical properties of cubic zinc blende ZnS have been studied using ab-initio approach. Plane-wave pseudopotential method within the basis of the first-principles density functional theory (DFT) and dispersion-corrected density functional theory (DFT-D) were done base on the implemented in CASTEP code. Structural parameters calculated were in good agreement with available experimental results. This study used the Generalized Gradient Approximation GGA-PBE and GGA-PBESOL to calculate the electronic properties and it is found that the results exhibit similar band structure qualitatively with the results calculated using LDA. Comparative study of results obtained for DFT and DFT-D showed that dispersion-corrected density functional theory (DFT-D) calculations may describe optical properties of a material better depending on the dispersion level.

Keywords: Zinc blende, Zinc Sulphide, DFT, DFT-D, Electronic and Optical properties

1. Introduction

There are three basic polymorphs of Zinc Sulphide (ZnS) namely the cubic zinc blende (zb), the hexagonal wurtzite (W) and the rarely observed cubic rock salt (RS). The main crystallographic form of ZnS are the cubic zinc blende (also known as sphalerite) and hexagonal wurtzite. The Strukturbericht symbol for zinc blende (zb) is B3 while that of wurtzite is B4. ZnSe, BeS and CdS are other examples of compound that shares the zinc blende (zb) B3 Strukturbericht symbol while ZnO, BeO, CdS and GaN are other examples of compound with wurtzite (W) B4 Strukturbericht symbols [1, 2]. Much attention has been given to both theoretical and experimental study of ZnS over the years due to its wide range of applications in photo sensing devices, electronic displays, laser application and photo catalytic application [3-6]. The lattice parameters for sphalerites (zinc blende) are $a=b=c=5.4093\text{\AA}$, $\alpha=\beta=\gamma=90^\circ$, cell volume = 158.279\AA^3 as given in the experimental result of Skinner [7]. Sphalerites Zinc Sulphide (ZnS) has cubic structure with $Z=4$ and space group name F-43m and space group number 216. The Wyckoff atomic position for Zn is 4a and S is 4c [2, 7]. Sphalerite ZnS has a face centered cubic (FCC) lattice structure. Its atoms have the coordinates of $T_d^2 - F\bar{4}3m$. [2]. Dispersion-corrected DFT are the usual DFT calculation where additional energy term introduced to the existing DFT functional. The dispersion correction energy term is a relatively simple function of interatomic distances and contain adjustable parameters that are fitted to conformational and interaction energies computed using Complete basis set limit extrapolation. Because the dispersion correction is an add-on term it does not directly alter the wavefunction or any other molecular property. Geometry optimizations with dispersion correction often change the geometry of the system since the dispersion correction influences the forces acting on the atoms. Dispersion corrections can lead to significant improvements in accuracy and the computational cost associated with dispersion corrections are negligible [8, 9].

2. Computational Methodology

The primitive unit cell of zb ZnS is shown in Fig.1. as obtained for the Wyckoff positions 4a (0 0 0; $\frac{1}{2}$ $\frac{1}{2}$ 0; $\frac{1}{2}$ 0 $\frac{1}{2}$; 0 $\frac{1}{2}$ $\frac{1}{2}$, or 0 0 0 FC) for Zinc atoms and 4c ($\frac{1}{4}$ $\frac{1}{4}$ $\frac{1}{4}$; $\frac{1}{4}$ $\frac{3}{4}$ $\frac{3}{4}$; $\frac{3}{4}$ $\frac{1}{4}$ $\frac{3}{4}$; $\frac{3}{4}$ $\frac{3}{4}$ $\frac{1}{4}$, or $\frac{1}{4}$ $\frac{1}{4}$ $\frac{1}{4}$ FC) for Sulphur atoms. Detail Wyckoff positions for all materials in the space group 216 is shown in Table 1. [2, 10]. The Computational method used in this study encompasses the popular density functional theory (DFT) with Perdew Burke Ernzerhof (PBE) [11] and PBESOL [12]

Correspondence Author: Olayinka A.S., Email: akinola.olayinka@edouniversity.edu.ng, Tel: +2348062447411

Transactions of the Nigerian Association of Mathematical Physics Volume 9, (March and May, 2019), 99 – 106

functionals as implemented in CASTEP code[13, 14] with the plane wave basis set cut-off of 395eV with $8 \times 8 \times 8$ k-point sampling. Optimization of the lattice parameters was done for bulk parameters of zb-ZnS using Broyden-Fletcher-Goldfarb-Shanno (BFGS) scheme[15] in order to determine the accuracy of the modelling by comparing calculated parameters to experimental results. The Pulay density mixed method was used to calculate the ground state energy which was set to 2×10^7 eV per atom. Relaxations were performed in two steps: First, with constant volume to optimize atomic positions in the lattice. Second, with unconstrained volume, to determine equilibrium bulk parameters and reference energies. The bulk modulus which measures the response in pressure, or resistance to a uniform compression, due to a change in the volume relative to the equilibrium, is calculated for zb-ZnS using Murnaghan's equation of state[16]

$$\mathbf{B} = -\mathbf{V} \frac{\partial \mathbf{P}}{\partial \mathbf{V}} = \mathbf{V} \frac{\partial^2 \mathbf{E}}{\partial \mathbf{V}^2} \quad (1)$$

where E is the total energy as a function of its volume V, P is the pressure and B the bulk modulus evaluated at the minimum of E. Self-consistent calculations were performed at room temperature for different k-point mesh, with proper weights in the irreducible Brillouin zone. The k-points were chosen along the high symmetry points in the Brillouin zone. Dispersion-corrected density functional theory (DFT-D) calculation was also carried out to compare the DFT and DFT-D calculated electronics and optical properties.

The complex dielectric function, $\epsilon(\omega)$ is useful in calculating the optical properties of solid (Ambrosch-Draxl and Sofo, 2006). It is defined as

$$\epsilon(\omega) = \epsilon_1(\omega) + i \epsilon_2(\omega) \quad (2)$$

where $\epsilon_1(\omega)$ is the real part and $\epsilon_2(\omega)$ is the imaginary part of dielectric function, which is mainly related to the electronic structure of a compound. Other optical constants, such as the refractive index $n(\omega)$, extinction coefficient $k(\omega)$, optical reflectivity $R(\omega)$, absorption coefficient $\alpha(\omega)$, energy-loss spectrum $L(\omega)$, and complex conductivity function $\sigma(\omega)$, can be gained from the complex dielectric function $\epsilon(\omega)$.

The imaginary part of dielectric function describes electronic absorption of materials while the real part relates to the electronic polarizability of materials. The real part of the complex dielectric function $\epsilon_1(\omega)$ can also be evaluated from the imaginary part $\epsilon_2(\omega)$ through the famous Kramer's Kronig relationship[17].

The imaginary part of the dielectric constant $\epsilon_2(\omega)$ which is given as part of equation (2) is related to the electronic band structure as given [6, 18].

$$\epsilon_2(\hbar\omega) = \frac{2e^2\pi}{\Omega\epsilon_0} \sum_{c,v} \sum_k \left| \langle \psi_k^c | \hat{u} \cdot r | \psi_k^v \rangle \right|^2 \delta(E_k^c - E_k^v - \hbar\omega) \quad (3)$$

where Ω is the volume of the elementary cell, vector u represents the polarization direction of the electric field of the incident photon, v represents the valence band while c represents the conduction band, k represents the reciprocal lattice vector, and ω represents the frequency of the incident photon while \hbar represents the normalised Planck constant. $\langle \psi_k^c | \hat{u} \cdot r | \psi_k^v \rangle$ represents the matrix elements that determine the probabilities of excitations of electrons occurring from the energy levels in the valence band (E_k^v) to the energy levels in the conduction band (E_k^c) i.e. interband transitions.

In real life computation, a broadening parameter Γ is introduced assuming a Drude-like shape for the intraband contribution $\epsilon_{ij}^{\text{(intraband)}}(\omega)$ can then be expressed as:

$$\text{Im} \epsilon_{ij}^{\text{(intraband)}}(\omega) = \frac{\Gamma \omega_{pl:ij}^2}{\omega(\omega^2 + \Gamma^2)} \quad (4)$$

$$\text{Re} \epsilon_{ij}^{\text{(intraband)}}(\omega) = 1 - \frac{\omega_{pl:ij}^2}{(\omega^2 + \Gamma^2)} \quad (5)$$

where $\omega_{pl:ij}$ is the plasma frequency.

The real part of the optical conductivity is then given as

$$\text{Re} \sigma_{ij}(\omega) = \frac{\omega}{4\pi} \text{Im} \epsilon_{ij}(\omega), \quad (6)$$

the loss function is

$$L_y(\omega) = -\text{Im} \left(\frac{1}{\epsilon_y(\omega)} \right), \quad (7)$$

and the reflectivity at normal incidence

$$R_{ii}(\omega) = \frac{(n-1)^2 + k^2}{(n+1)^2 + k^2} \tag{8}$$

where n and k are respectively the real part(refractive index) and imaginary part (extinction coefficient) of the complex reflectivity.

$$n_{ii}(\omega) = \sqrt{\frac{|\epsilon_{ii}(\omega)| + \text{Re} \epsilon_{ii}(\omega)}{2}} \tag{9}$$

$$k_{ii}(\omega) = \sqrt{\frac{|\epsilon_{ii}(\omega)| - \text{Re} \epsilon_{ii}(\omega)}{2}} \tag{10}$$

Then the absorption coefficient is given by

$$\alpha_{ii}(\omega) = \frac{2\omega k(\omega)}{c} \tag{11}$$

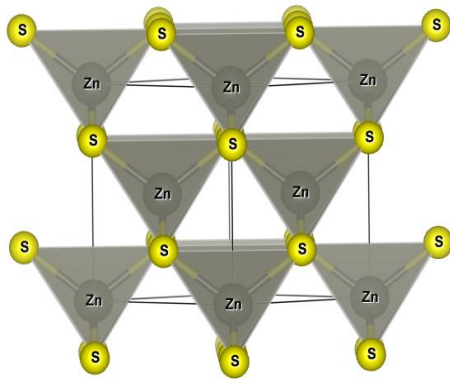


Fig. 1: The unit cell of zb-ZnS Structure

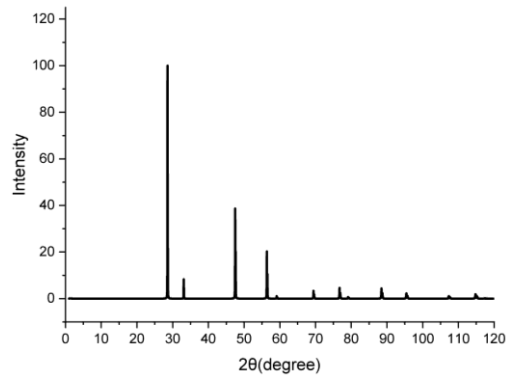


Fig. 2: Powder Diffraction Pattern for zb-ZnS

Table 1: The Wyckoff positions of the group 216 (F-43m) showing 4a and 4c position for Zn and S atoms respectively [10]

Multiplicity	Wyckoff letter	Site symmetry	Coordinates
			(0,0,0) + (0,1/2,1/2) + (1/2,0,1/2) + (1/2,1/2,0) +
96	i	1	(x,y,z) (-x,-y,z) (-x,y,-z) (x,-y,-z) (z,x,y) (z,-x,-y) (-z,-x,y) (-z,x,-y) (y,z,x) (-y,z,-x) (y,-z,-x) (-y,-z,x) (y,x,z) (-y,-x,z) (y,-x,-z) (-y,x,-z) (x,z,y) (-x,z,-y) (-x,-z,y) (x,-z,-y) (z,y,x) (z,-y,-x) (-z,y,-x) (-z,-y,x)
48	h	.m	(x,x,z) (-x,-x,z) (-x,x,-z) (x,-x,-z) (z,x,x) (z,-x,-x) (-z,-x,x) (-z,x,-x) (x,z,x) (-x,z,-x) (x,-z,-x) (-x,-z,x)
24	g	2.m m	(x,1/4,1/4) (-x,3/4,1/4) (1/4,x,1/4) (1/4,-x,3/4) (1/4,1/4,x) (3/4,1/4,-x)
24	f	2.m m	(x,0,0) (-x,0,0) (0,x,0) (0,-x,0) (0,0,x) (0,0,-x)
16	e	.3m	(x,x,x) (-x,-x,x) (-x,x,-x) (x,-x,-x)
4	d	-43m	(3/4,3/4,3/4)
4	c	-43m	(1/4,1/4,1/4)
4	b	-43m	(1/2,1/2,1/2)
4	a	-43m	(0,0,0)

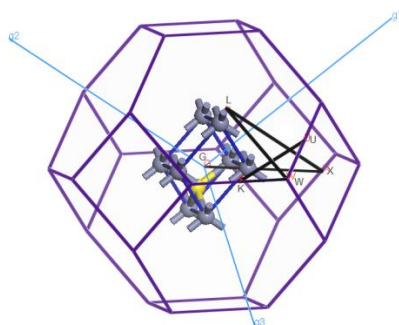


Fig. 3: Brillouin Zone high symmetry direction (Γ -X-L-W-K-U) for Face Centred Cubic (FCC)zb-ZnS.

3. Results and Discussion

3.1 Electronic Properties

Electronic Band Structure and Density of State (DOS) of zb-ZnS as shown in figure 4 is the calculated band structure along the high symmetry directions of the first Brillouin zone (Γ -X-L-W-K-U) adopted from figure 3. The corresponding density of state (DOS) is attached to the side of the band structure. The Generalized Gradient Approximation (GGA) calculation was done with Exchange-correlation functional PBESOL and direct band gap of 2.007eV was obtained at Γ point in figure 4 as against the band gap of 1.973eV obtained for rev PBE functional. The horizontal dashed line indicates the position of the Fermi energy (E_F) level. Dispersion-corrected DFT gave a band gap of 1.851eV. Calculated Density of states (DOS) for zb-ZnS agreed with band gap obtained from band structure.

Table 2 shows calculated band gaps of zb-ZnS as compared with other theoretical as well as experimental ones. Band gap obtained compared favourably with other theoretical results [19, 20]but when compared with experimental results[21, 22], there was band gap underestimation which is consistent with density function theory limitations.

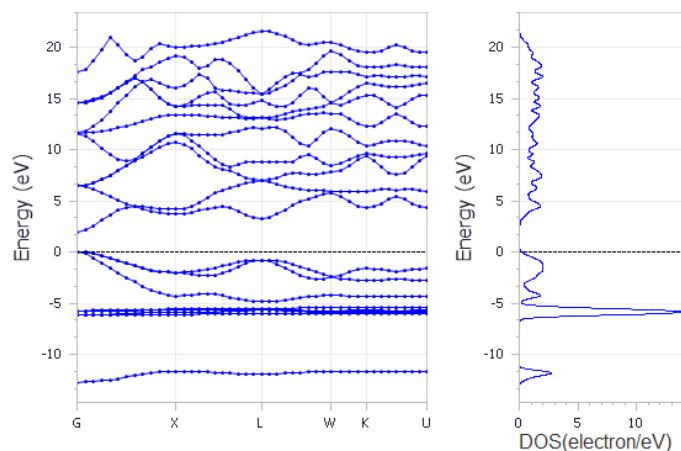


Fig. 4: Electronic Band Structure and Density of State (DOS) of zb-ZnS along the high symmetry directions of the first Brillouin zone (Γ -X-L-W-K-U). Direct band gap of 1.973eV was obtained at Γ point

Table 2: Calculated band gaps of zb-ZnS

Band Gap, E_g (eV)	Potential / Method	Reference
1.973	GGA-DFT revPBE	This Work
2.007	GGA-DFT PBESOL	
1.851	DFT-D	
2.03	GGA	[19]
1.65	LDA	[20]
1.84	LDA	[19]
3.723	Photoluminescence	[21] [21]
3.70	Thermal evaporation	[22]

3.2 Optical Properties

Optical properties calculated in this work include; dielectric function, $\epsilon(\omega)$, absorption, $\alpha(\omega)$, optical conductivity, $\sigma(\omega)$, energy loss spectrum, $L(\omega)$, reflectivity, $R(\omega)$ and refractive coefficients ($n(\omega)$ and $k(\omega)$). $n(\omega)$ and $k(\omega)$ are respectively the real and imaginary part of the complex refractivity respectively. $n(\omega)$ and $k(\omega)$ are respectively the refractive index and extinction coefficient. All optical properties investigations were done within the chosen energy range of 0 – 40eV using both DFT and DFT-D. The results are presented in figures 5 – 10. Figure 5 shows the calculated complex dielectric function as a function of frequency for zb-ZnS for both DFT and DFT-D calculations. The imaginary part of the frequency dependent dielectric function and real part are shown. The optical peak is obtained for the imaginary part frequency dependent dielectric function at 6.11eV and 6.02eV for DFT and DFT-D calculations respectively.

Dielectric function values of 6.18 for DFT and 6.31 for DFT-D are measured for the real part, $\epsilon_1(\omega)$. These values suggest the materials capability to be as an electron acceptor, hence, DFT-D calculation shows a higher potential as an electron acceptor.

Figure 6 shows the calculated absorption spectra, $\alpha(\omega)$ for zb-ZnS. Absorption spectra, $\alpha(\omega)$ define materials ability to harvest or trap electromagnetic radiation or incident light. Absorption values of 281940.41cm^{-1} and 280773.55cm^{-1} were measured at optical peaks of 8.56eV and 8.36eV for DFT and DFT-D respectively. DFT-D calculated absorption showed higher capability of light absorption compared to DFT calculation.

Calculated reflectivity spectra, $R(\omega)$ is shown in figure 7 while figure 8 showed refractive coefficients for zb-ZnS. At 0eV, reflectivity values of 0.181 was measured for DFT calculation and 0.185 for DFT-D calculation. Optical peaks of reflectivity occurred at 9.10eV and 9.01eV respectively for DFT and DFT-D with corresponding reflectivity values of 0.465 and 0.474.

DFT-D exhibited maximum reflectivity of 0.474 with differential reflectivity of 0.009 over DFT computed reflectivity. Refractive index, $n(\omega)$ and extinction coefficient, $k(\omega)$ spectra are shown in figure 8. Optical conductivity spectra for DFT and DFT-D calculations are shown in figure 9. Computed values for refractive indices, extinction coefficient and optical conductivities are summarized in Table 3.

Figure 10 shows the energy loss function $L(\omega)$ of zb-ZnS. This parameter describes the energy loss when an electron passing through a medium. Two distinctive peaks were recorded for loss function at energy 17.64eV and 19.70eV for DFT-D calculation while the distinctive peaks recorded DFT calculation were at energy 17.82eV and 20.31eV.

Table 3: Calculated refractive indices, extinction coefficients and Optical conductivities

Energy (eV)	Refractive Index (n)	Methods
0.0	2.51	DFT-D
3.79	3.05	
5.29	3.03	
0.0	2.49	DFT
3.89	3.03	
5.48	3.01	
Energy (eV)	Extinction coefficient (k)	
6.28	2.04	DFT-D
8.06	2.11	
6.40	1.99	DFT
8.16	2.09	
Energy (eV)	Conductivity (1/fs)	
6.04	7.56	DFT-D
7.62	6.80	
6.14	7.51	DFT
7.73	6.93	

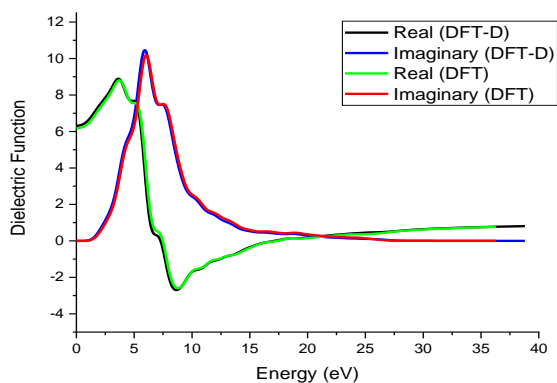


Fig. 5: Calculated Dielectric Function for zb-ZnS.

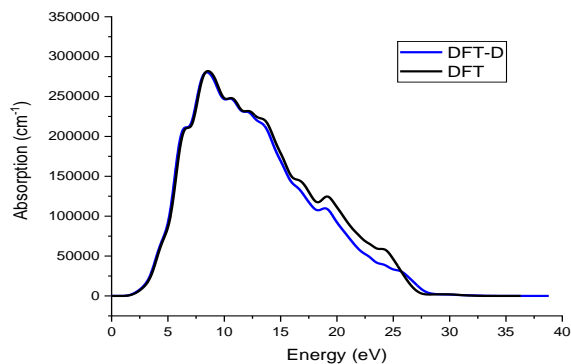


Fig. 6: Calculated Absorption for zb-ZnS

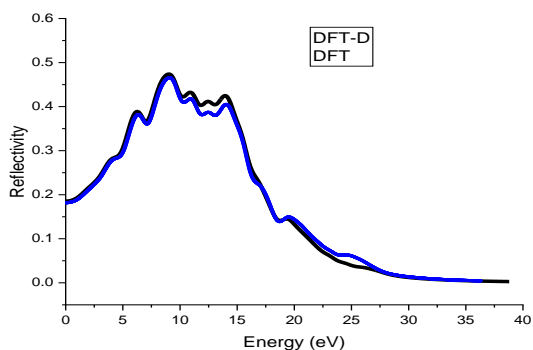


Fig. 7: Calculated for Reflectivity zb-ZnS

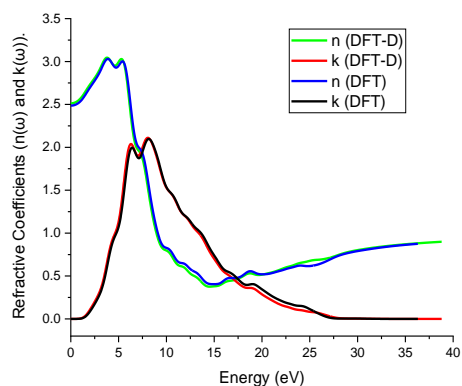


Fig. 8: Calculated Refractive Coefficient for zb-ZnS

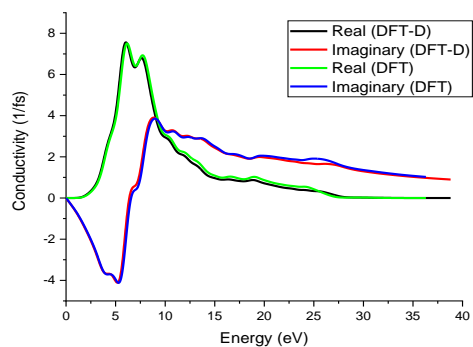


Fig. 9: Calculated Conductivity for zb-ZnS

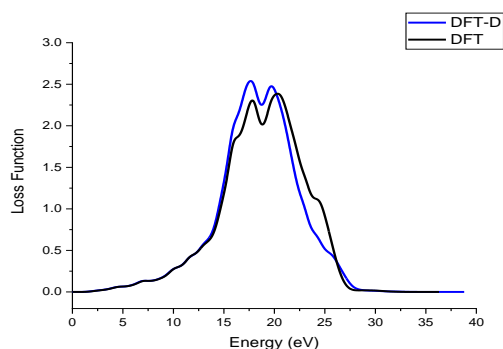


Fig. 10: Calculated Loss function for zb-ZnS

4.0 Conclusion

Electronic and optical properties of zb-ZnS were computed using plane wave method within DFT and DFT-D. Generalized Gradient Approximation with PBE and PBESOL parameterization were employed to calculate the exchange correlation energy and potential. Our results are compared with the already done experimental and theoretical works. Results obtained compared favourably with previous calculations. Comparison of the result obtained from DFT and DFT-D shows minimal improvements of DFT result by the introduction of dispersion to DFT.

References

- [1] La Porta, F.A., Ferrer M. M., Santana Y. V. B., Raubach C. W., Longo V. M., Sambrano J.R., Longo E., Andrés J., Li M. S., Varela J. A. , *Synthesis of wurtzite ZnS nanoparticles using the microwave assisted solvothermal method*. J. Alloys Compd, 2013. **555**: p. 153-159.
- [2] Tilley, R., *Crystal and Crystal Structures*. 2006: John Wiley & Sons Ltd, West Sussex, England.
- [3] La Porta, F.A., et al., *A DFT Study of Structural and Electronic Properties of ZnS Polymorphs and its Pressure-Induced Phase Transitions*. Journal of the American Ceramic Society, 2014. **97**(12): p. 4011-4018.
- [4] Raubach, C.W., et al., *Photocatalytic activity of semiconductor sulfide heterostructures*. Dalton Transactions, 2013. **42**(31): p. 11111-11116.
- [5] Yang, J., et al., *Controllable photoluminescent–magnetic dual-encoded wurtzite ZnS: Cu²⁺ Mn²⁺ nanowires modulated by Cu²⁺ and Mn²⁺ ions*. Journal of Alloys and Compounds, 2013. **574**: p. 240-245.
- [6] Olayinka, A., et al., *Ab initio study of electronic and optical properties of nitrogen-doped rutile TiO₂*. International Journal of Modern Physics B, 2019. **33**(06): p. 1950036.
- [7] Skinner, B.J., *Unit-cell edges of natural and synthetic sphalerites*. 'American Mineralogist, 1961. **46**: p. 1399-1411.
- [8] Grimme, S., et al., *A consistent and accurate ab initio parametrization of density functional dispersion correction (DFT-D) for the 94 elements H-Pu*. The Journal of chemical physics, 2010. **132**(15): p. 154104.
- [9] Jensen, J.H., *Molecular modeling basics*. 2010: CRC Press.
- [10] Aroyo, M.I., Perez-Mato J.M., Capillas C., Kroumova E., Ivantchev S., Madariaga G., Kirov A. and Wondratschek H. , *Bilbao Crystallographic Server I: Databases and crystallographic computing programs*. Z. Krist., 2006. **221**(1): p. 1527.
- [11] Zhang, Y. and W. Yang, *Comment on “Generalized gradient approximation made simple”*. Physical Review Letters, 1998. **80**(4): p. 890.
- [12] Perdew, J.P., et al., *Restoring the Density-Gradient Expansion for Exchange in Solids and Surfaces*. Physical Review Letters, 2008. **100**(13): p. 136406.
- [13] Clark, S.J., et al., *First principles methods using CASTEP*. Zeitschrift für Kristallographie-Crystalline Materials, 2005. **220**(5/6): p. 567-570.
- [14] Segall, M., et al., *First-principles simulation: ideas, illustrations and the CASTEP code*. Journal of Physics: Condensed Matter, 2002. **14**(11): p. 2717.
- [15] Fische, T., *Almlof J. J. Phys. Chem.*, 1992. **1992**: p. 96.
- [16] Murnaghan, F., *The compressibility of media under extreme pressures*. Proceedings of the National Academy of Sciences, 1944. **30**(9): p. 244-247.
- [17] Ambrosch-Draxl, C. and J.O. Sofo, *Linear optical properties of solids within the full-potential linearized augmented planewave method*. Computer Physics Communications, 2006. **175**(1): p. 1-14.
- [18] Wooten, F., *Optical Properties of Solids (Academic, New York, 1972)*. Google Scholar, 1972: p. 115.

- [19] Luo, W., et al., *Quasiparticle band structure of ZnS and ZnSe*. Physical Review B, 2002. **66**(19): p. 195215.
- [20] Agrawal, B.K., P. Yadav, and S. Agrawal, *Ab initio calculation of the electronic, structural, and dynamical properties of Zn-based semiconductors*. Physical Review B, 1994. **50**(20): p. 14881.
- [21] Tran, T., et al., *Photoluminescence properties of ZnS epilayers*. Journal of applied physics, 1997. **81**(6): p. 2803-2809.
- [22] Geng, B., et al., *Structure and optical properties of periodically twinned ZnS nanowires*. Applied physics letters, 2006. **88**(16): p. 163104.